Russian Geology and Geophysics © 2020, V.S. Sobolev IGM, Siberian Branch of the RAS
Vol. 61, No. 4, pp. 396–411, 2020 *DOI:10.15372/RGG2019147* *Geologiya i Geofizika*

Petrological and Geochemical Characteristics and Age of the Rocks of the Yllymakh Massif (Aldan Shield, Southern Yakutia)

E.A. Vasyukova[a,b,] ✉, A.V. Ponomarchuk[a], A.G. Doroshkevich[a,c]

[a] *V.S. Sobolev Institute of Geology and Mineralogy, Siberian Branch of the Russian Academy of Sciences, pr. Akademika Koptyuga 3, Novosibirsk, 630090, Russia*

[b] *Novosibirsk State University, ul. Pirogova 1, Novosibirsk, 630090, Russia*

[c] *Geological Institute, Siberian Branch of the Russian Academy of Sciences, ul. Sakhyanovoi 6a, Ulan-Ude, 670047, Russia*

Received 30 July 2018; received in revised form 29 May 2019; accepted 28 August 2019

Abstract—The Yllymakh massif is one of the Mesozoic ring intrusions widespread in Central Aldan. The alkaline rocks composing it are greatly diverse in composition. Based on the obtained petrological, geochemical, and geochronological data, we have recognized three groups of rocks, marking the different phases of the massif formation. The rocks of two groups resulted from the fractionation of rock-forming minerals (pyroxene and plagioclase) and accessory apatite, which is reflected in the composition trends in the variation diagrams and in the REE patterns. Assimilation of the crustal material also significantly contributed to the diversity of rock-forming melts, which is evidenced from the increase in $^{87}Sr/^{86}Sr$ from group to group. At the same time, the ε_{Nd} value is steadily extremely low throughout the study area (on average, –13.5). The obtained Ar–Ar geochronological data indicate three independent stages of the massif formation: 140.0 ± 1.9, 130.0 ±1.9–131.0 ± 2.4, and 125.0 ± 1.9 Ma, which are close in time to the evolution stages of other Mesozoic massifs in Aldan.

Keywords: alkaline rocks, Sr–Nd isotope composition, Ar–Ar age, Yllymakh massif, Central Aldan

INTRODUCTION

The Aldan Shield is the largest exposure of the basement of the Siberian craton to the surface with a clearly revealed block structure. An activation in the Mesozoic of the neighbouring Verkhoyano-Chukotskaya and Mongol-Okhotsk fold areas, which are the southern and southeastern edges of the paleocontinent, caused a tectonic-magmatic activation of the Aldan Shield with characteristic intraplate magmatism (Kochetkov, 2006) and formed the Aldan high-potassium alkaline province (Maksimov, 1975). According to (Yarmolyuk et al., 1995, 2000), this manifistation of Mesozoic magmatism on the Siberian craton could be explained by the influence of a sub-lithospheric "superplume in the mantle" in the form of intensive rifting and intraplate volcano-plutonic activity associated with the formation of trought deflections, depressions and grabens. On the other hand, the appearance of the Mesozoic tectonomagmatic activity on the Aldan Shield in (Khomich et al., 2014, 2015; Khomich and Boriskina, 2016) was associated with the process of dehydration of a subducted oceanic plate due to a subsequent upwelling of asthenospheric material, to deformations in the lithosphere, and to a manifestation of multi-stage plume magmatism.

The Mesozoic alkaline rocks of the Aldan Shield are characterized by an exceptional variety of compositions, features of tectonic and geological occurrence conditions. Using the approaches of formational analysis, researchers selected the three most widespread types of the formations within this shield: leucite–alkali–syenitic, monzonite–syenite and medium acidic granitoids types (Maksimov, 1975). The nature of the correlation of formations across the shield allows us to distinguish the spatial lateral zonation: in the west, a leucite-alkali syenite formation dominates, in the central part it is supplemented by a monzonite–syenite one, and in the east and south-east a formation of acidic granitoids prevails.

According to the current geological data (Explanatory note…, 2016), the following stages of Mesozoic magmatism could be distinguished within the Central Aldan area:

– the Late Triassic and the Early Jurassic stages, which are absent in our study area;

– the Middle-Late Jurassic stage (the Tommotian volcanic leucite-alkaline trachytic and Verkhneseligdar hypabyssal syenite–porphyritic complexes);

– the Late Jurassic and Early Cretaceous stage (the Aldan plutonic fergusite-alkaline-syenitic and Lebedinsky plutonic monzonite–syenite–granite complexes);

✉ Corresponding author.
E-mail address: lenav@inbox.ru (E.A. Vasyukova)

– the Early Cretaceous stage (Tobuksky hypabyssal vogesite-minette complex, Kurungsky complex of potassium feldspar metasomatites, Koltykonski hypabyssal syenite-porphyric complex and Elkonsky hypabyssal alkaline syenitis–alkaline granite complex).

The main, most active stage of Mesozoic magmatism occurred during the Late Jurassic epoch – the beginning of the Early Cretaceous epoch. Manifestations of this stage are the Aldan fergusite–alkaline–syenitic complex and Lebedinsky monzonite–syenite–granite complex, which intruding into the Aldan complex into. Intrusions of these two complexes are concentrated in their largest volumes within relatively large (20–100 km^2) polyphase plutons, which often have a concentric structure. These include also the studied Yllymakh massif. Here, the Aldan complex is manifested in the form of numerous semiconical intrusions, stocks, dikes, and the Lebedin complex is presented in the form of small stocks near the main body of the Yllymakh massif.

In each complex, there are several phases, whose ages and relationships between, which were determined through geological methods. The first phase includes the rocks of a potassium affinity (malignites, pseudoleucite syenite–porphyries, shonkinites, biotite porphyrites); the second one includes the rocks of a sodium–potassium affinity (nepheline, analcime syenites, alkaline syenites, feldspathoid syenite–porphyries).

G.K. Shnay and M.P. Orlova (1977) published ages, which cover a relatively significant range between – 165 and 131 Ma. The age of the earliest rocks in the massif – of malignites, melanocratic, pseudoleucite and nepheline syenites, and shonkinites, are in the range between 165 and 158 Ma. Monzonites, epileucite phonolites and trachytes were formed in the interval 152–142 Ma. The formation of the massif was completed by the introduction of alkali syenites, granosyenites and aegirine granites in the range between 133 and 131 Ma. For comparison, we should compare the available geochronological data on the Yllymakh massif with precise data for some other massifs of the Central Aldan region obtained recently. The earliest rocks of the Ryabinovyi massif, according to Ar-Ar analysis, have an age of 144.8±5 Ma, and lamprophyre dikes date back to a range between 129 and 125 Ma (Borisenko et al., 2011). The same interval of magmatism, between 147 and 120 Ma, can be confirmed by Rb-Sr and U-Pb isotope systems (Shatov et al., 2012, 2017). The main boundaries of the formation of the alkaline frame of the Inagli massif have close time frames: crystallization of the dunite core margin – clinopyroxenites is dated no later than 145.8 ± 3.2 Ma; and the formation of the differentiated alkaline ring of the massif occurred in the range between 133 and 128 Ma: the age of crystallization of the melanocratic syenites is 133.2 ± 2.2 Ma, of the monzonite–porphyries – 130 ± 2.4 Ma, of the leucocratic syenites – not later than 128.2 ± 4.4 Ma, shonkinites – not later than 129 ± 1.4 Ma (Ponomarchuk et al., 2019). Dikes and sills of monzonite porphyries, emplaced both on the area of the Inagli massif and in the immediate vicinity, have U-Pb age between 130 and 133 Ma (Ibrahimova et al., 2015), which is confirmed by Ar-Ar data – 130 ± 2.4 Ma (Ponomarchuk et al., 2019).

The first data on the sequence of formation of the Yllymakh complex are given in (Bilibin, 1947) on the basis of geological relationships of the rocks. The earliest magmatic formations are alkaline basaltoids (biotite pyroxenites) of the Tommotian complex. They form rare necks within the studied massif. Their age is determined by the fact that they are breaking terrigenous deposits Yukhta and Duray formations and, at the same time, they are under the influence of contact alterations from later moderately alkaline intrusions of the Lebedinsky and the Aldan complexes. These relationship are observed next to the hills Lebediny, Spirin, Piramid, Geologichesky, Yakokutsky volcano-plutons. The absolute age determined by the K-Ar method using the bulk rock composition is 187.7 ± 2.3 Ma (Maximov, 2003), and by the KFsp method – 166 ± 6 Ma (Eremeev, 1984).

It is obvious that for geodynamic reconstruction and characteristics of the sources of materials it is necessary to determine the exact age of formation of rocks of the Yllymakh massif. The actual absence of modern geochronological data on the object of study determines the need for geochronological studies, so this article presents the results of datings of all varieties of rocks in the massif.

The interest in the Yllymakh massif rose in the geological literature repeatedly. But each of the works was devoted only to some separate aspect that characterized the massif, and did not give a general, integral petrological description. For example, in the monograph of Yu.A. Bilibin (1947) there is a geological description. For the first time, the description of the variety and composition of rocks of the Yllymakh massif has been presented. In a series of works written by G.P. Dvornik with co-authors (Ugryumov et al., 1996, 2001; Ugryumov and Dvornik, 1997; Dvornik and Elyuev, 2001; Dvornik, 2016), the metasomatic processes imposed on the rocks of the Yllymakh massif and its ore content are considered in detail. The authors identified the stages, determined the zoning of gold-porphyry mineralization in metasomatites of potassium alkaline massifs, also, they indicated the criteria for identifying ore-bearing bodies and prospects for the development of potassium alkaline massifs as a gold-porphyry type of mineralization. An assessment of physical and chemical conditions of olivine shonkinite formation in the Yllymakh massif according to thermobarogeochemical studies is presented in (Panina et al., 2011).

As we demonstrate, none of these works does not give an overall picture of the formation of the spectrum of rocks of the massif, but only explain one or another aspect. In addition, for the rocks of the Yllymakh massif, there is no isotope-geochemical information that is needed to characterize the sources of description for the studied rocks. The available few isotope-geochemical data on the late Mesozoic alkaline complexes of the Aldan shield indicate the predominance of the enriched mantle component in the formation of

source chambers (Bogatikov et al., 1994; Mitchell et al., 1994; Pervov et al., 1997; Vladykin, 2005). It is obvious that to assess the existence of an enriched lithospheric mantle under the Aldan shield, it is necessary to obtain the missing isotopic and geochemical information on a statistically significant number of alkaline massifs, including the main Yllymakh massif.

This article presents the results of petrological, geochemical, isotopic and geochronological studies of rocks of the Yllymakh massif (alkali syenite–porphyries, alkali syenites, pseudoleucite syenites, nepheline syenites and alkali granites). The question of time and genetic relations, sources of materials, the problem of formation and evolution of rock-forming alkaline melt is discussed.

BRIEF GEOLOGICAL DESCRIPTION

The Yllymakh massif is located in the southern part of the Aldan shield, and is a part of the Central Aldan ore district. The geological position of the Yllymakh massif is determined by its location on the border of the Verkhne-Jakokutsky graben the immediate neighbourhood of the intersection node major faults that were reactivated in the Mesozoic – northwest striking Yukhtinsky, which is the largest in the Central Aldan and the Yllymakh fault (Fig. 1) (Dvornik, 2016).

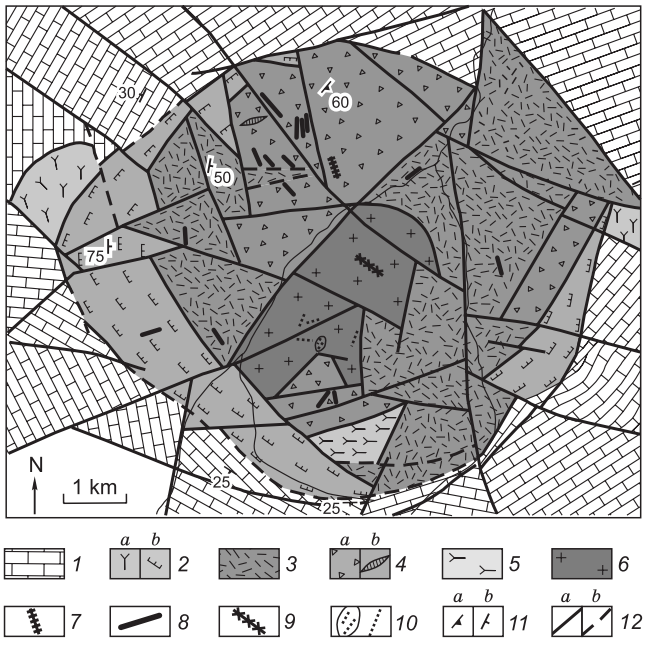

Fig. 1. Geological sketch map of the Yllymakh alkaline volcano-plutonic massif (according to Bilibin, 1947; Shnai and Orlova, 1977). *1*, Early-Cambrian marmorized, Cambrian dolomites and linestones; *2*, monzonites (*a*), malignites (*b*); *3*, epileucite phonolites, trachytes, their tuffs; *4*, nepheline and pseudoleucite syenites (*a*) and pegmatites of nepheline syenites (*b*); *5*, alkali nepheline-containing syenites (pulaskites); *6*, granites and granosyenites; *7*, foid microsyenites; *8*, alkali syenite–porphyre; *9*, granite- and granosyenite–porphyre; *10*, quartz; *11*, trachytes (*a*) and attitude trace elements (*b*); *12*, faults determined (*a*) and inferred (*b*).

Intrusive bodies belonging to the Yllymakh massif are located among monotonous strata of sedimentary rocks – dolomites of Cambrian and Vendian-Cambrian age, underlain by Archean granites.

The Yllymakh volcano-pluton has the shape of an elongated oval with a size of 5.1×4.4 km, with evident, zonation and concentric structure. Intrusive contacts between different types of rocks and the presence of xenoliths of earlier rocks in the later rocks indicate multiple, impulsive intrusion of portions of magma (Bilibin, 1958).

The earliest rocks are alkali rocks-monzonites and malignites, as is described in (Bilibin, 1958; Shnai and Orlova, 1977). These rocks form two large, separated areas in the western and eastern parts of the massif. The main, largest part of the massif is formed by large stocks of nepheline and alkali syenites. Rocks were intensively modified by secondary processes (e.g. muscovitisation, carbonisation). The alkali syenites are cut by numerous dikes of solvsbergites and alkali granites. Even younger are the monzonites–syenites, manifested in the form of separate bodies, which intrude earlier rocks, as well as located in two separate small stocks, located in the east and in the west of the main body. In the inner zone, there is an isometric body of aegirine granites and eruptive breccias of these rocks.

At the moment, there are many points of view both on the diversity and on the age of the rocks composing the massif. Therefore, in addition to these rocks, there are within the massif some dikes of pseudoleucite tinguaites, a pulaskite stock, small bodies and dikes of alkali syenite porphyries. It is also worth noting the forms of quartz presence, from small individual grains and small evenly distributed rocks (this is typical for the northern part of the bunch), to large clusters and nests. One of the largest segregations has an oval shape in terms of size 20×30 m, composed of pure quartz, forming elongated columnar crystals with an irregular section. Due to the cracks of the jointing, these crystals break easily and form fragments with length up to several decimeters. The presence of any ore minerals could not be detected inside the quartz clusters. Near the southern contact of the stock aegirine granites were found, which gradually make a transition to a pure pegmatitic quartz.

We have selected a collection of samples of rocks of the Yllymakh massif. Due to the inaccessibility of the outcrops of the object under study, the collection does not include the entire variety of rocks described in literary sources. However, it allows to draw preliminary conclusions, anticipating a more detailed study.

ANALYTICAL METHOD

$^{40}Ar/^{39}Ar$ dating was carried out using monomineral fractions, which were selected manually under a binocular microscope from the fraction between 0.3 and 0.1 mm of the crushed sample. Irradiation of samples was conducted in a

cadmium-plated channel of the research reactor of the VVR-K type (boiling water reactor) at the Research Institute of Nuclear Physics (Tomsk). The neutron flux gradient for the irradiation period did not exceed 0.5% in the sample size. As a monitor, a standard K/Ar sample of muscovite MSA-11 (Branch Standard Sample (OSO) No. 129-88) prepared by the All-Soviet Union Research Institute of Mineral Resources of the Ministry of Geology of the USSR (ASURIMR) in 1988 was used. For its calibration as a $^{40}Ar/^{39}Ar$ monitor, international standard samples of a muscovite Bern 4m and a biotite LP-6 were used (Baksi et al., 1996). According to the results of calibration, the mean age of the muscovite MSA-11 was considered to be 311.0±1.5 Ma (Travin, 2016). The value of the total decay rate ^{40}K, according to (Steiger and Jager, 1977), was taken to be 5.543×10^{-10} year^{-1}.

Blank test by definition ^{40}Ar (10 min at 1200 °C) did not exceed 5×10^{-10} ncm^3. An argon purification was performed using Ti – and ZrAl-SAES-getters. An additional purification was carried out using a quartz appendix immersed in liquid nitrogen. The isotopic composition of argon was measured on the mass spectrometer Noble gas 5400 made by "Micromass" (England). The following coefficients were used to correct for the isotopes ^{36}Ar, ^{37}Ar, ^{40}Ar obtained under an irradiation of Ca, K: $(^{39}Ar/^{37}Ar)_{Ca}$ = 0.000891 ± 0.000005, $(^{36}Ar/^{37}Ar)_{Ca}$ = 0.000446 ± 0.000006, $(^{40}Ar/^{39}Ar)_{K}$ = 0.089 ± 0.001. Special attention was paid to the control of the isotope discrimination factor by measuring the portion of purified atmospheric argon. The average value of the ratio $^{40}Ar/^{36}Ar$ for the period of measurements was 295.5 ± 0.5. The sample was heated in a quartz reactor placed in a resistive furnace. The dating was carried out by the method of step heating. The temperature control was carried out by means of a chromel–aluminum thermocouple. The temperature control accuracy was ±1 °C.

The isotopic composition of oxygen in minerals was determined at the Geological Institute (Ulan-Ude) on the Finnigan MAT 253 mass spectrometer using the laser fluorination method (Sharp, 1990). The samples were heated by 100W CO_2 laser in BrF_5 atmosphere. International standard materials were used as calibration samples: quartz NBS-28 (9.65‰; n = 10) and biotite NBS-30 (5.11‰; n = 15). The garnet standard UWG-2 (5.88‰) was analyzed in the process of each experiment to ensure greater accuracy. Based on these data and the reproducibility of repeated measurements, the error value of $\delta^{18}O$ of the samples did not exceed 0.2‰.

A determination of the content of Sr and Rb isotopes was made at the laboratory of isotope analytical methods at V.S. Sobolev Institute of Geology and Mineralogy (Novosibirsk, analyst – V.Yu. Kiseleva). In the subsample of the sample as large as about 0.1 grams, crushed to 0.1 mm, we added 5–10 ml of a mixture of concentrated hydrofluoric and perchloric acids, with a ratio of 4:1. A decomposition was carried out at a temperature of about 230 °C, then the sample was evaporated to wet salts, then for the decomposition of insoluble fluorides, we added again successively concentrated $HClO_4$, HNO_3 70% and twice HCl 30%.

At the end of the decomposition process, the excess acids were removed by evaporation to a dry state, and the dry residue was transferred to chlorides. The chlorides were dissolved in 2N hydrochloric acid, the solution was centrifuged and the centrifuge was transferred to the prepared ion exchange column.

To determine the contents of Rb and Sr, the analysis procedure was similar, only a tracer enriched with ^{85}Rb and ^{84}Sr was added to the subsample of the sample.

The separation of rubidium and strontium was carried out on quartz chromatographic columns by ion exchange chromatography. The chromatographic columns with a volume of 1–2 ml were filled with the cation exchanger Dowex AG W50×8 having grain size 200–400 mesh. The eluent is 2N HCl.

Measurements were taken using the multicollector mass spectrometer MI 1201AT. The chromatographic allocated strontium in the form of nitrate was applied to the rhenium ribbon with size 20×0.7×0.03 mm and was measured in a double-ribbon mode using also rhenium ionizers.

The accuracy of the determination of the Sr isotope ratios was controlled by a parallel measurement in each series of samples of the ISG-1 isotope standard with an isotope ratio of strontium of 0.71732±10 and a content of Rb 145 ppm, Sr 227 ppm.

Measurements of the isotopic composition of neodymium and concentrations of Sm and Nd were carried out on the mass spectrometer Finnigan MAT 262 in static two-band mode using rhenium and tantalum ribbons at the Geological Institute of the Kola Science Centre (Apatity). The average value of the ratio $^{143}Nd/^{144}Nd$ in the La Jolla standard for the measurement period was 0.511835±18 (n = 15). The error in $^{147}Sm/^{144}Nd$ relationships is equal to 0.3% (2σ) – this is the mean value among seven measurements of the BCR standard. The error of measurement of the Nd isotope composition in the individual analysis did not exceed 0.005%. Blank intralaboratory contamination for Nd was equal to 0.3 ng, and for Sm was equal to 0.06 ng. The accuracy of Sm and Nd concentrations was equal to ± 0.5%. The isotopic ratios were normalized to $^{146}Nd/^{144}Nd$ = 0.7219 and then converted to the accepted ratio $^{143}Nd/^{144}Nd$ in the La Jolla standard = 0.511860. In calculating the $\varepsilon_{Nd}(T)$ values and the T (DM) model ages, the modern values of CHUR (Bouvier et al., 2008) and DM (Goldstein and Jacobsen, 1988) were used.

An ICP-MS analysis of Rb, Sr, Y, Zr, Nb, Cs, Ba, REE, Th and U in rocks of the massif, host strata and metasomatites, were carried out using the ELEMENT spectrometer with an ultrasonic nebulizer U-5000AT + at the laboratory of isotope analytical methods at V.S. Sobolev Institute of Geology and Mineralogy (Novosibirsk, analyst – I.V. Nikolaeva). The research methodology is described in (Nikolaeva et al., 2008).

PETROGRAPHIC AND PETROCHEMICAL CHARACTERISTICS OF ROCKS

Pseudoleucite syenites. A holocrystalline rocks, with an evident porphyry structure. Phenocrysts are represented by crystals of potassium feldspar and epileucite. The latter has the form of large areas of subisometric or irregular shape. The ground mass is microlithic, composed of potassium feldspar, and of small biotite scales. The accessory minerals are titanites, replaced by leucoxene, and apatite. The rocks are often albitized, carbonatized. A ferruginization also is typically occuring, this is expressed in the form of limonite and hematite.

Nepheline syenites. A holocrystalline rocks with porphyry structure, and an ophitic structure of the ground mass. The main rock-forming minerals are clinopyroxene (30%), potassium feldspar (50%), nepheline (10%), there also is a small amount of biotite. Accessory mineralization is represented by apatite. In the phenocrysts, they include clinopyroxene with a characteristic zoning – from colorless in the central part to greenish in the marginal part. The clinopyroxene in the ground mass is colored green with different intensity. The potassium feldspar has in the ground mass a form of idiomorphic elongated crystals. The nepheline in the rock forms large oikocrysts with inclusions of potassium feldspar. The biotite occupies the intergranular space in the form of xenomorphic grains. The apatite is idiomorphic with slightly smoothed edges.

Alkali syenites. The rock is holocrystalline, uniformly grained with a massive texture. The syenite is composed of aegirine–augite (up to 15%), plagioclase (up to 15%), potassium feldspar (up to 65%), quartz (up to 5%), phlogopite (single grains). The accessory minerals are represented by titanite, apatite. The feldspar forms large (up to 3.6 mm) idiomorphic crystals with expressed crystallographic facets. Typical for these, we can find perthites, confined to the central part of crystals. The plagioclase and aegirine–augite are represented by subidiomorphic grains of smaller (up to 2 mm) size. Xenomorphic quartz nodes occupy the interstices between the grains. The titanite has the form of xenomorphic grains and clusters of fairly large size (up to 0.8 mm).

Alkali granites. A holocrystalline rock, with inequigranular massive textures. It is composed of potassium feldspar, quartz and clinopyroxene with aegirine–augite composition. The largest are the quartz crystals (up to 4 mm). They have an expressed crystallographic faceting. Between them, there are subdiomorph grains of feldspar (up to 2 mm) with a characteristic microcline lattice and a weakly manifested pelitization. In the interstices, and the edge zones of the growth of quartz, there are abundant small grains of aegirine-augite with an elongated crystal habit (Fig. 2).

PETROLOGICAL AND GEOCHEMICAL CHARACTERISTICS OF ROCKS

The chemical composition of the studied rocks is given in Table 1. According to the content of SiO_2 rocks, with the exception of alkali granites, they belong to the group of intermediate rocks. By the amount of alkalis ($K_2O + Na_2O$) exceeding 10%, the studied rocks are alkaline, by the content of K_2O (>4%) and by the ratio of K_2O/Na_2O, they belong to the group of high-potassium rocks with potassium and potassium-sodium type of alkalinity (Fig. 3). All studied rocks are divided into three groups according to the silica content. However, a further analysis of the data confirmed the validity of this division and other characteristics.

In the **first** group of rocks, including alkali and feldspar syenites, the amount of SiO_2 varies from 50 to 56 wt.%. According to the sum of ($Na_2O + K_2O$), they belong to the alkali-type, as evidenced by the presence of feldspathoids (leucite, nepheline). In addition, the rocks are characterized by a higher concentrations of MgO, Fe_2O_3, TiO_2, P_2O_5, Ba, Sr compared to others. Most of the variation diagrams (Fig. 4) the points of rock compositions of this group have a clear negative correlation with the silica content (MgO–CaO–Fe_2O_3–MnO–P_2O_5–SiO_2). Based on the values of the Na_2O/K_2O coefficient, the rocks of the first group have a potassium affinity of alkalinity. According to the nomenclature based on mineral composition, they belong to the family of feldspar or alkali syenites.

The **second** group includes medium rocks of potassium-sodium affinity. The content of SiO_2 in them varies from 60 to 70 wt.%. According to the mineral composition, they vary from nepheline-containing to quartz-containing rocks, and belong to the family of syenites. On the variation diagrams for most petrogenic components, there was a correlation: mostly positive, as well as for the composition points of the first group. The exception was Al_2O_3, whose content decreased with increasing silicicity (Fig. 3).

The **third** group, which included aegirine granites and their pegmatites, clearly differed in the content of most elements, forming an independent cluster in the diagrams (Fig. 3). However, the rocks retain the potassium type of alkalinity and geochemical similarity, which will be discussed in more detail below (Fig. 3).

The MgO content does not exceed 1 wt.% for most samples, but in rare cases reaches 4 wt.%. In the MgO–Fe_2O_3 diagram, the composition points of the studied rocks fit into a linear trend, which indicates in favor of the assumption of fractional crystallization within each group (Fig. 3). Taking into account the spread of petrogenic elements in the variation diagrams, it is especially well seen for the rock compositions from the first group, it is possible to assume the fractionation of rock-forming (plagioclase and pyroxene), as well as accessory (apatite) minerals. The rocks with a higher magnesium content are also characterized by a higher TiO_2 content.

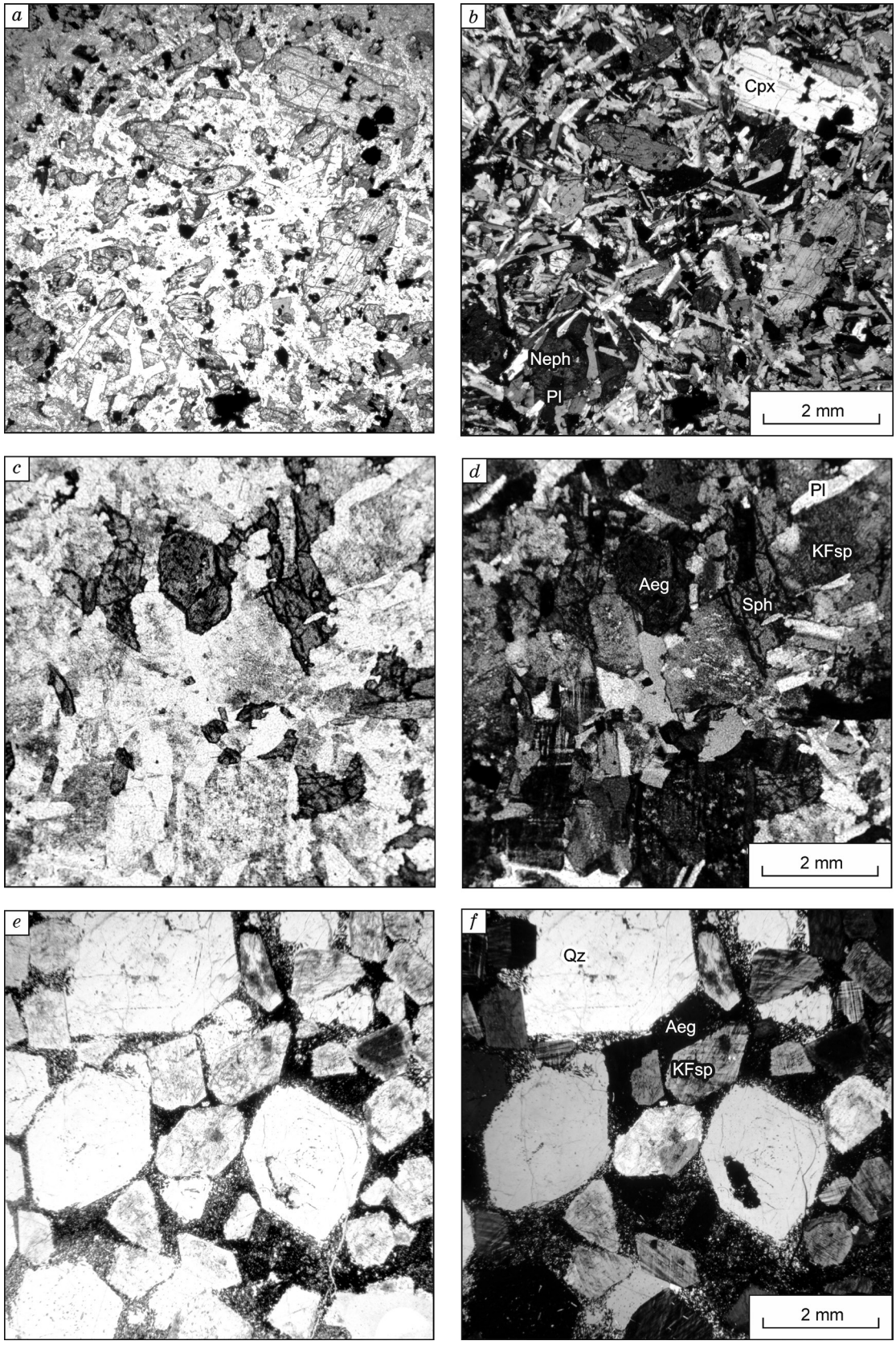

Fig. 2. Nepheline syenite in transmitted light (*a*) and in crossed nichols (*b*); alkali syenite in transmitted light (*c*) and in crossed nicols (*d*); alkali granites in transmitted light (*e*) and in crossed nicols (*f*).

Table 1. The content of primary (in wt.%) and dispersed elements (in ppm) in the rocks of the Yllymakh massif

Component	2136*	2140	2142	2154	2144	2146	2134	2148	2150	2152	2156	2160	2164	2166	2172
	Foid syenites						Alkali syenites							Alkali granites	
	First group						Second group							Third group	
SiO_2	52.01	55.53	55.9	50.44	53.02	55.33	67.34	67.35	60.75	62.21	64.69	68.62	68.95	82.99	85.63
TiO_2	0.98	0.53	0.65	0.98	0.96	0.67	0.16	0.19	0.47	0.46	0.39	0.16	1.03	0.29	0.16
Al_2O_3	14.14	19.45	17.84	14.05	16.27	18.32	15.8	14.25	18.17	14.81	16.18	13.55	13.51	6.17	5.97
Fe_2O_3	10.62	6.09	5.98	10.62	8.18	5.64	2.96	3.28	4.18	5.62	3.57	3.32	3.4	3.61	1.87
MnO	0.17	0.13	0.09	0.17	0.17	0.12	0.07	0.06	0.13	0.09	0.09	0.07	0.19	0.09	0.03
MgO	4.01	0.16	0.7	4.1	2.31	1.44	0.07	0.22	0.42	1.34	0.41	0.19	0.3	0.25	0.11
CaO	6.34	0.67	1.38	6.55	3.8	1.39	0.31	0.5	1.34	2.61	1.24	0.63	0.7	0.27	0.15
Na_2O	3.18	9.61	6.26	2.8	3.13	2.01	7.12	3.52	7.74	6.07	7.01	1.72	4.07	0.92	0.46
K_2O	7.29	6.4	9.47	7.57	8.58	11.8	5.11	9.17	5.8	6.31	5.72	11	7.41	5.01	5.08
P_2O_5	0.82	0.02	0.1	0.83	0.45	0.26	0.02	0.04	0.07	0.18	0.08	0.08	0.04	0.01	0.01
BaO	0.43	0.02	0.17	0.42	0.65	0.66	0.03	0.02	0.04	0.12	0.15	0.02	0.08	0	0
SO_3	0	0.12	0.22	0	0.11	0.1	0.04	0	0.33	0.07	0.05	0	0	0	0
LOI	0.22	0.52	0.5	0.93	1.7	1.56	0.23	1.55	0.57	0.16	0.05	0.24	0.11	0.11	0.1
Total	100.3	99.31	99.35	99.54	99.41	99.36	99.31	100.27	100.08	100.12	99.7	99.75	99.85	99.87	99.67
Ti									2649.3	2589.4	2128.4	847.9	5962.8	1532.3	851.1
V	224.3	100.6	193.7	224.6	216.9	94.9	74.6	392.3	125.3	175.4	139.4	576.3	168.9	951.5	450.8
Cr	42.4	14.5	13.8	43.5	17.5	11.1	8.6	20.3	10.2	43.8	10.3	31.0	25.3	45.7	30.2
Mn									1033.2	693.6	642.1	544.5	1521.8	752.7	257.5
Co	27.8	2.8	5.2	25.3	17.3	9.6	1.2	1.6	3.1	5.8	3.0	2.2	3.3	3.0	1.2
Ni	23.3	4.7	5.3	18.8	5.5	7.7	28.6	8.6	0.0	8.7	3.2	4.5	4.5	5.8	3.3
Cu	109.7	21.8	37.0	98.8	38.0	23.7	15.9	17.3	51.2	121.8	20.8	65.0	136.6	39.2	30.6
Zn	96.1	92.0	51.2	40.7	126.5	108.5	68.0	36.3	38.9	11.1	21.8	17.4	43.9	22.1	15.1
Rb	151.6	249.6	125.6	137.5	163.1	254.0	129.8	152.7	163.6	132.2	106.6	140.1	107.2	53.6	55.9
Sr	1930.3	1122.5	1880.7	1874.8	2632.7	1555.8	66.3	117.4	822.6	348.3	719.4	85.6	337.3	14.4	6.6
Y	20.8	206.8	8.5	20.8	23.1	13.7	8.1	3.1	19.9	17.0	8.2	5.6	34.3	2.7	1.4
Zr	140.5	361.8	187.7	125.0	310.6	231.3	183.1	116.5	334.2	258.3	172.0	319.9	744.7	111.0	76.1
Nb	6.9	18.6	7.4	5.6	13.2	11.6	12.1	4.9	11.4	9.2	10.6	7.4	53.7	2.0	1.4
Mo	2.2	0.8	1.1	1.9	0.6	0.6	1.1	0.8	0.8	1.6	2.9	1.1	2.7	1.2	1.2
Cs	2.7	2.8	1.2	1.4	4.2	5.1	1.2	0.4	2.0	0.4	1.0	0.3	0.2	0.2	0.2
Ba	3607.9	155.7	1443.8	3484.8	5125.3	5269.2	265.7	164.4	325.0	1060.8	1198.1	187.7	671.0	21.6	15.6
La	39.2	402.6	25.0	39.6	43.0	25.9	22.9	12.7	58.9	26.4	24.7	9.9	68.5	8.7	4.9
Ce	74.0	695.8	42.7	74.0	70.8	43.6	30.8	16.7	78.3	50.1	39.4	16.8	156.8	6.8	5.8
Pr	9.5	73.9	5.1	10.1	8.2	5.1	2.6	1.3	8.0	6.2	3.8	1.5	10.2	0.9	0.5
Nd	38.7	243.5	18.6	38.0	31.1	19.3	6.9	3.6	23.6	21.1	11.7	4.8	27.9	2.6	1.3
Sm	7.7	43.6	3.1	7.3	5.4	3.6	1.1	0.5	4.2	4.0	1.9	0.7	4.7	0.3	0.2
Eu	2.1	13.6	0.9	1.9	1.5	1.0	0.4	0.1	1.2	1.3	0.6	0.2	1.5	0.1	0.1
Gd	6.7	42.0	2.6	7.4	5.0	3.2	1.0	0.5	4.3	4.5	2.3	0.9	5.5	0.5	0.2
Tb	0.9	7.0	0.4	0.9	0.8	0.5	0.2	0.1	0.6	0.6	0.3	0.1	0.8	0.1	0.0
Dy	4.9	43.2	2.0	4.7	4.8	3.0	1.2	0.4	3.5	3.4	1.7	0.8	5.4	0.3	0.2
Ho	0.9	9.1	0.4	0.9	1.0	0.6	0.3	0.1	0.8	0.7	0.3	0.2	1.3	0.1	0.0
Er	2.5	25.8	1.2	2.4	2.8	1.9	1.0	0.4	2.5	2.1	1.0	0.7	4.3	0.3	0.2
Tm	0.4	3.7	0.2	0.4	0.5	0.3	0.2	0.1	0.4	0.4	0.2	0.2	0.8	0.1	0.0
Yb	2.3	20.0	1.2	2.1	2.8	1.8	1.6	0.7	2.9	2.4	1.4	1.1	6.0	0.5	0.3
Lu	0.4	2.8	0.2	0.3	0.4	0.3	0.3	0.1	0.5	0.3	0.2	0.2	0.9	0.1	0.1
Hf	4.0	12.2	5.9	4.5	7.9	5.5	5.5	4.4	12.3	9.3	6.1	10.1	28.8	4.5	3.5
Ta	0.4	0.6	0.6	0.5	0.5	0.5	0.4	0.2	0.6	0.4	0.5	0.3	2.0	0.1	0.1
Pb	24.4	70.1	52.5	23.0	62.2	18.9	113.7	57.8	72.2	13.0	97.7	93.7	705.1	1011.4	564.2
Th	5.3	54.0	4.2	4.0	14.0	6.9	12.8	6.4	28.1	10.3	12.7	6.2	95.7	60.7	88.3
U	1.6	12.1	1.6	1.2	3.2	2.4	4.1	2.5	12.9	4.6	3.2	5.1	18.8	5.6	7.4

*Sample number

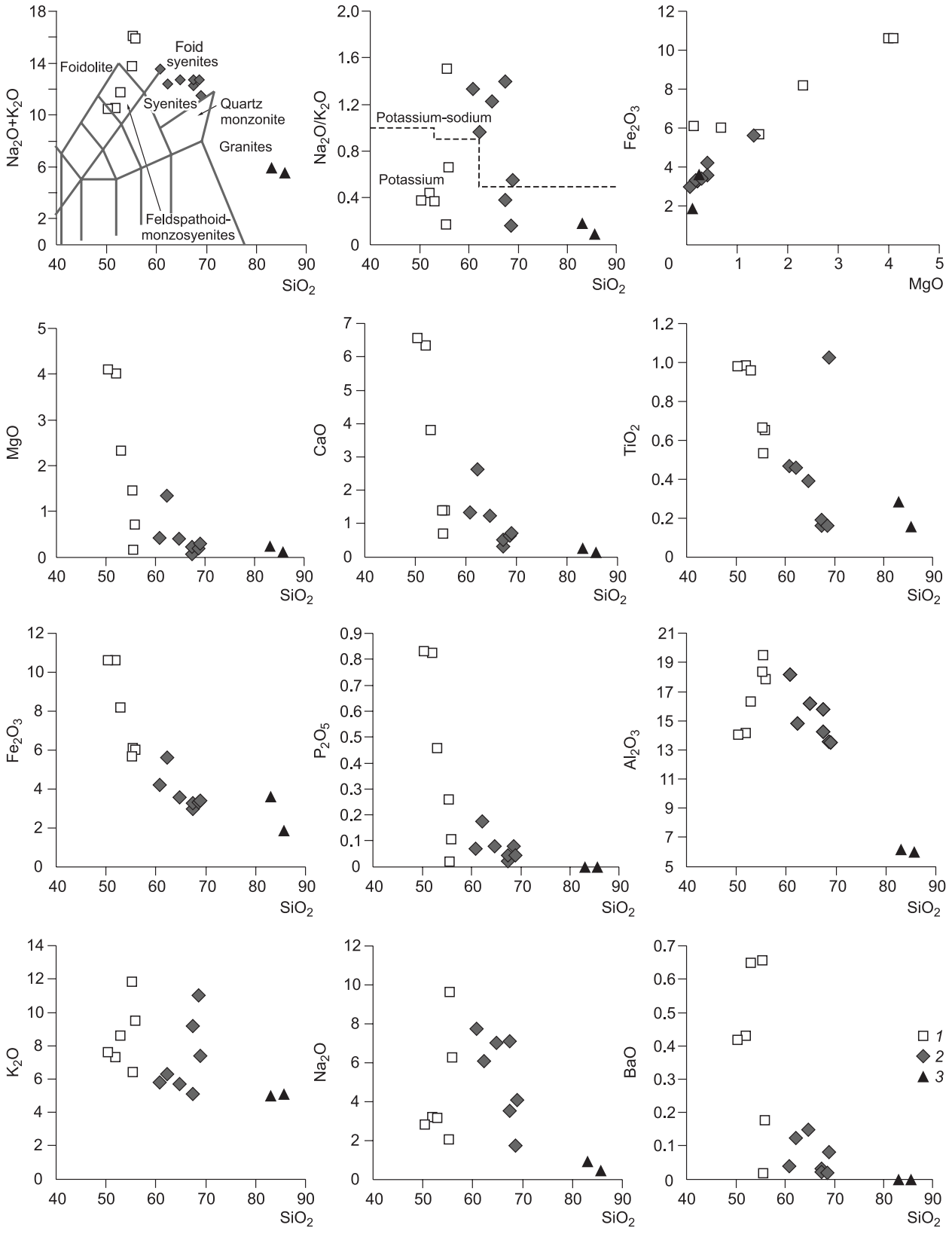

Fig. 3. Petrochemical and geochemical characteristics of the rocks of the Yllymakh massif. The borders on the TAS-diagram are displayed in wt.%. *1*, rocks of the first group (foid syenites); *2*, rocks of the second group (alkali syenites); *3*, rocks of the third group (aegirine granites).

The mineral composition correlates with the chemical one: the rocks with elevated P_2O_5 are characterized by high levels of apatite, and in the rocks with high K_2O content, we found pseudoleucite.

For geochemical studies, rocks representing three different groups were selected. The content of rare and rare-earth elements for representative samples is presented in Table 1. The construction of the distribution spectra of the contents of rare and rare-earth elements, normalized to rare-earth metals, showed the similarity of the absolute values, the general form, the direction of the graphs, and the position of anomalies.

A normalized to rare-earth metals content of rare elements in the rocks of the first group vary widely, for individual elements differing by an order of magnitude, while maintaining the shape of a graph. Multielement spectra for rocks of the second group are very close, almost completely repeating each other in a narrow range of values. The lowest content of rare elements (Fig. 4), except Th, U, Pb, is in alkali granites. Also in Fig. 4, a complementarity of the spectra of granites and syenites of the second group is clearly visible (the anomalies have opposite signs for elements such as Ba, Th, Sr, Ti). Other anomalies: positive for Zr, Hf, Pb and negative for Ta, Nb – they are observed in all the selected groups.

The graphs of all rocks have similar values for Rb, K, Hf, Zr, Ti. A minimum value of Ba for granites and rocks of the second group (alkali and feldspar syenites), in contrast to the maximum in the graphs of rocks of the first group (syenites), is directly related to the amount of alkaline feldspar.

The graphs of the distribution of rare-earth elements normalized to the primitive mantle are close in absolute values in the region of light and heavy rare-earth elements and differ in the number of medium rare-earth elements. The configuration of curves for granites and feldspar syenites is characterized by a relatively gentle slope and a U-shape. Such a form can be caused by heavy enrichment or depletion in the area of medium rare earths. According to previous researchers, the graphs of the content rare-earth elements in olivine shonkinites, assuming the earliest rocks of the Yllymakh massif, are within the field of compositions of the studied samples, but have a relatively flat shape with a gentle slope. However, it is worth noting that the content of lanthanides from the middle part of the spectrum is definitely correlated with the content of silica (Fig. 5). The distribution spectra of the rare-earth elements for alkali and feldspar syenites have a smooth, flat shape with a negative slope (La/Yb~12).

For rare earth spectra, the same trends are observed as for multi-element spectra: a narrow intra-group range of values for granites and the group of feldspar and alkali syenites, between which there are graphs of the distribution of elements for feldspar syenites. It should be noted that the spectra within each group are subparallel to each other, which is especially evident for feldspar syenites. In the Eu-Gd Region, spectra for all rocks show a slight instability in the direction of decreasing Eu and increasing Gd.

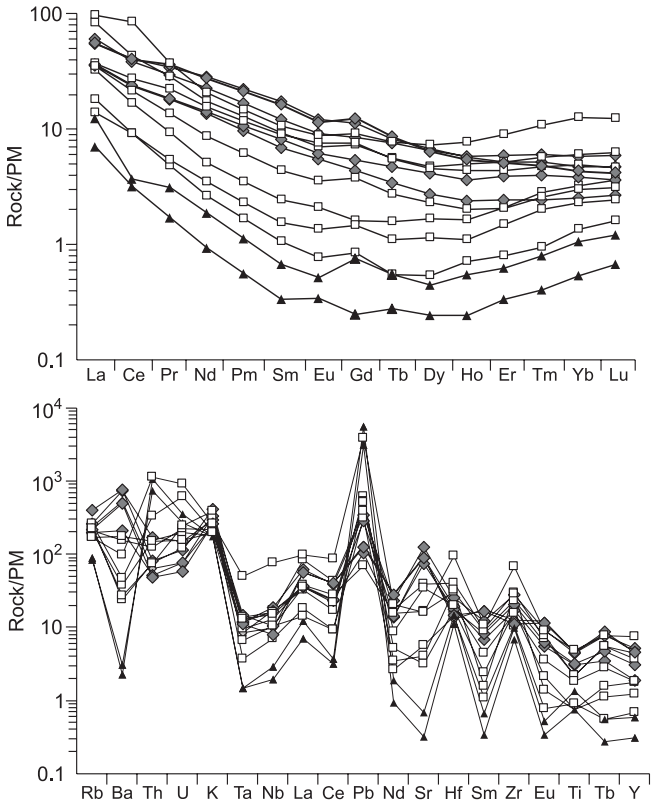

Fig. 4. Distribution graphs of the contents of rare (*a*) and rare-earth (*b*) elements normalized on primitive mantle (PM) by (McDonough and Sun, 1995) in the rocks of the Yllymakh massif.

Ar-Ar DATING RESULTS

For a geochronological research, we selected main types of rocks on the Yllymakh massif.

We performed an Ar-Ar isotopic analysis of phlogopite from a nepheline syenite (sample 2136). The obtained age spectrum of the mineral consisted of seven steps (Fig. 6; Table 2). The last five steps meet the criteria for the age plateau. At least three successive age steps were within the error interval ±3σ and represented at least 70% of the ^{39}Ar isolated during measurements (Fleck et al., 1977). The Ca/K spectrum of the sample was characterized by a low Ca/K ratio in the range between 0.05 and 0.1. The amount of the isolated ^{39}Ar included in the age plateau was equal to 90%. The weighted average age of mineral formation on the age plateau is equal to 140±1.9 Ma. This value can be accepted as the closing time of the Ar-Ar isotope system in the phlogopite and therefore be considered as the crystallization age of nepheline syenites.

$^{40}Ar/^{39}Ar$ spectrum of feldspar from syenite (sample 2148), consists of eight steps (Fig. 6). Four steps meet the

Table 2. Results of age determination by $^{40}Ar/^{39}Ar$ method in rocks of the Yllymakh massif

T, °C	$^{40}Ar/^{39}Ar$	±	$^{38}Ar/^{39}Ar$	±	$^{37}Ar/^{39}Ar$	±	$^{36}Ar/^{39}Ar$	±	Age, Ma	±	Cumulative ^{39}Ar, %
Sample 2136, phlogopite (*J* = 0.003577 ± 0.000034, integrated age 135.3 ± 2.1 Ma)											
500	65.3	3.1	0.09	0.07	0.1	0.1	0.15	0.05	122.3	84.6	0.8
650	30.3	0.2	0.031	0.005	0.06	0.01	0.044	0.005	107.5	9.6	8.7
750	27.89	0.07	0.018	0.002	0.032	0.009	0.020	0.002	136.0	4.5	24.5
850	25.49	0.05	0.019	0.001	0.013	0.006	0.014	0.002	132.0	3.6	46.7
940	25.87	0.02	0.021	0.002	0.008	0.005	0.009	0.001	144.1	1.9	69.5
1030	28.18	0.04	0.028	0.002	0.020	0.008	0.020	0.001	138.2	2.8	90.1
1130	30.8	0.1	0.021	0.003	0.003	0.003	0.029	0.005	138.9	8.3	100.0
Sample 2156, feldspar (*J* = 0.003571 ± 0.000033, integrated age 130.1 ± 3.4 Ma)											
500	136.9	9.7	0.15	0.08	0.4	0.1	0.42	0.08	83.4	128.2	1.2
610	44.7	0.4	0.039	0.009	0.03	0.01	0.077	0.009	135.4	15.6	8.6
720	33.0	0.1	0.023	0.002	0.010	0.003	0.042	0.003	127.8	5.9	34.4
820	28.9	0.1	0.018	0.004	0.034	0.008	0.026	0.004	131.3	7.2	53.8
920	30.3	0.1	0.024	0.003	0.02	0.02	0.032	0.004	129.8	7.2	65.8
1030	28.25	0.02	0.022	0.004	0.007	0.006	0.025	0.001	130.0	1.9	79.3
1140	27.5	0.1	0.0198	0.0005	0.013	0.006	0.020	0.004	133.0	6.7	100.0
Sample 2148, feldspar (*J* = 0.003818 ± 0.000038, integrated age 131.4 ± 2.3 Ma)											
500	84.2	1.6	0.11	0.02	0.23	0.07	0.21	0.02	155.7	34.9	1.5
600	38.8	0.3	0.031	0.004	0.08	0.02	0.051	0.007	156.7	12.3	6.4
700	23.74	0.06	0.023	0.003	0.006	0.006	0.014	0.003	129.6	5.3	16.8
800	22.67	0.06	0.018	0.002	0.016	0.008	0.010	0.002	130.1	4.8	32.0
900	21.05	0.02	0.018	0.001	0.007	0.004	0.004	0.001	131.1	2.4	61.8
975	21.59	0.06	0.007	0.003	0.03	0.01	0.005	0.003	133.7	5.5	79.1
1050	22.38	0.07	0.020	0.004	0.03	0.02	0.015	0.003	119.5	5.9	89.3
1130	22.6	0.1	0.018	0.001	0.007	0.006	0.011	0.005	128.9	9.5	100.0
Sample 2166, feldspar (*J* = 0.004632 ± 0.000056, integrated age 132.4 ± 1.8 Ma)											
500	129.8	4.6	0.13	0.05	0.2	0.1	0.35	0.04	0.5	206.5	78.6
600	33.42	0.02	0.014	0.004	0.02	0.01	0.0424	0.0005	4.7	166.6	2.2
700	24.85	0.09	0.022	0.003	0.001	0.001	0.024	0.004	11.4	142.3	8.7
800	21.05	0.02	0.016	0.002	0.010	0.004	0.0126	0.0007	25.9	139.3	2.3
880	19.85	0.02	0.021	0.001	0.005	0.002	0.0099	0.0006	43.4	136.2	2.1
960	19.78	0.02	0.0196	0.0007	0.005	0.003	0.0144	0.0008	65.1	125.4	2.4
1040	20.16	0.02	0.0201	0.0007	0.009	0.003	0.0161	0.0007	85.0	124.4	2.2
1130	20.63	0.02	0.0176	0.0008	0.006	0.001	0.0173	0.0005	100.0	125.2	1.9

Note. Error interval ±2σ.

criterion of the age plateau and determine the weighted average age of the study sample – 131±2.4 Ma (Table 2). The amount of released ^{39}Ar corresponds to 80% of the total volume of ^{39}Ar. The Ca/K spectrum of the sample under consideration shows a fairly uniform Ca/K ratio (0.05–0.1) for the stages selected as the age plateau. Thus, the obtained age of 131±2.4 Ma corresponds to the age of closure of $^{40}Ar/^{39}Ar$ isotope system in feldspar and corresponds to the time of formation of syenites.

We performed Ar-Ar isotope studies of feldspar from trachyte (sample 2156), which shows an age range, consisting of seven steps (Fig. 6). At the same time, a reliable plateau of five stages is distinguished, the weighted average age of which is 130 ± 1.9 Ma (Fig. 6). The Ca/K spectrum of the sample under consideration shows homogeneously low Ca/K ratios in steps, excluding the first one. The pseudo-plateau generating steps comprise more than 90% of the allocated ^{39}Ar, so the resulting estimate of the age of feldspar may be taken at the time of its formation.

The $^{40}Ar/^{39}Ar$ age spectrum of aegirine from granite feldspar (rock sample 2166) consists of eight steps (Fig. 6; Table 2). It is difficult to distinguish the age plateau. The three

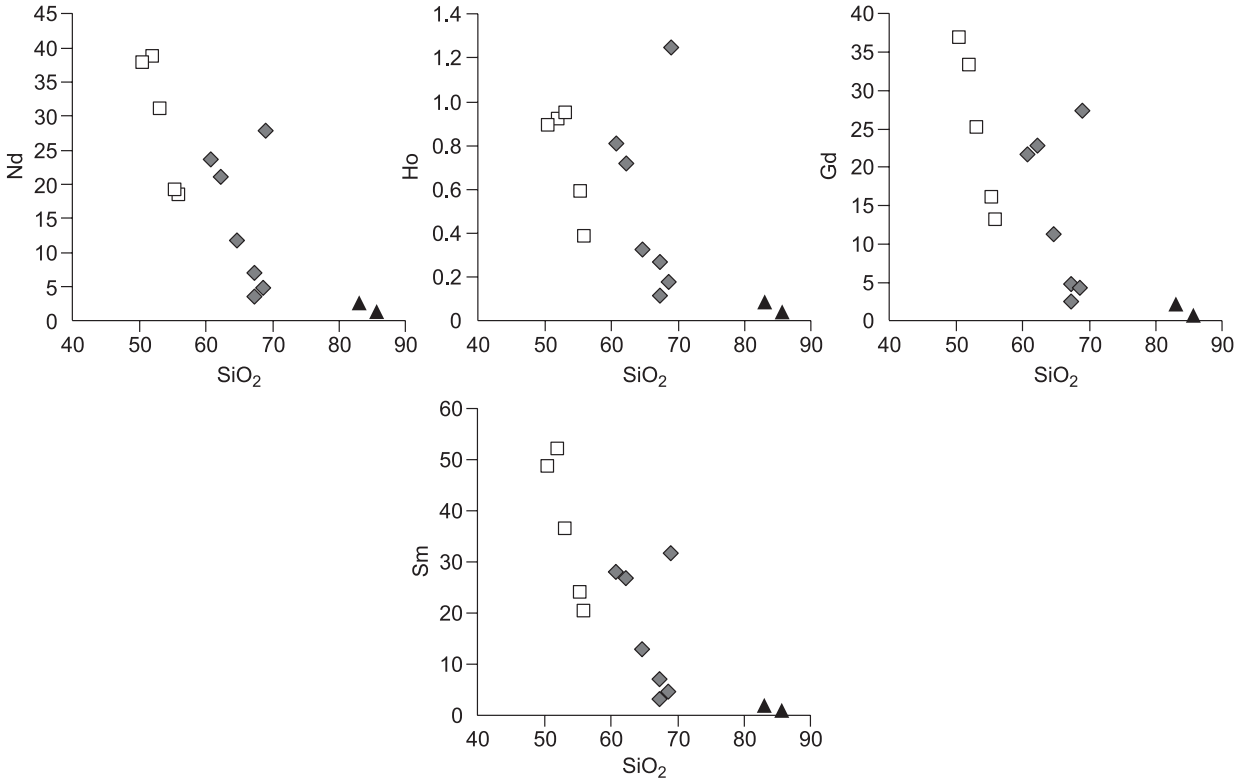

Fig. 5. Graphs of the ratio of the content of rare earth elements (ppm) of the middle part of the spectrum with the content of silica (wt.%). Symbols designation are the same as in Fig. 3.

high-temperature steps include only 60% of the released ^{39}Ar, with a requirement of 70% (Fleck et al., 1977). The stepped low-and medium-temperature part of the spectrum (Fig. 6) is probably related to the heterogeneity of the sample and a not high stability of the K-Ar isotope system in feldspar (closing temperature 125–350 °C). High-temperature steps, in turn, exhibited homogeneous isotopic characteristics that coincided with the error. Thus, the weighted average age of mineral formation is equal to 125 ± 1.9 Ma and can be accepted as the formation age. The Ca/K spectrum confirms the homogeneity of the ratio selected as the age table plate of the stages (Fig. 6). However, it is worth noting the low content of Ca in the rock as a whole (Table 1) and, as a consequence, a low signal of ^{37}Ar (Table 2), which makes it difficult to study the homogeneity of the sample.

ISOTOPIC (O, Sr-Nd) CHARACTERISTICS OF ROCKS

Oxygen isotopic composition. The values of the isotopic composition of oxygen in minerals in the rocks of the Yllymakh massif are given in Table 3. The $\delta^{18}O$ values in the feldspars from nepheline syenites fall in a narrow interval (7.1–8.4‰). The phlogopite in the nepheline syenites (rock sample 2136) shows a lighter isotopic composition equal to 6.1‰. The abnormally light composition of oxygen in the pyroxene of this sample (3.2‰) is noteworthy. Most likely, the source of the isotopic label was lost owing to secondary changes superimposed on pyroxene. The amphibole in the syenite (sample 2156) showed a low concentrations of heavy oxygen (5.8‰) compared to those in the feldspar (7.1‰), which corresponds to the ability to concentrate ^{18}O with different minerals (Epstein and Taylor, 1967; Chacko et al., 2001). In general, the obtained ^{18}O studied minerals fall within the range of values typical for igneous rocks (4.5–7‰ (Hoefs, 2009)).

Isotopic composition of Sr and Nd. The values of $^{143}Nd/^{144}Nd$ and $^{87}Sr/^{86}Sr$ are shown in Table 4 and in Fig. 7. According to the obtained geochronological data, the initial values of Sr and Nd were recalculated for the age of 130 Ma for samples 2140 and 2146, 140 Ma for samples 2134, and

Table 3. The isotopic composition of Oxygen in the rocks of the Yllymakh massif

Rock	Sample	Mineral	$\delta^{18}O_{SMOW}$, ‰
Foid syenites	2136	Feldspar	7.8
		Phlogopite	6.1
		Pyroxene	3.2
Alkali syenites	2148	Feldspar	8.4
»	2156	Feldspar	7.1
		Amphibole	5.8
		Matrix	8.9

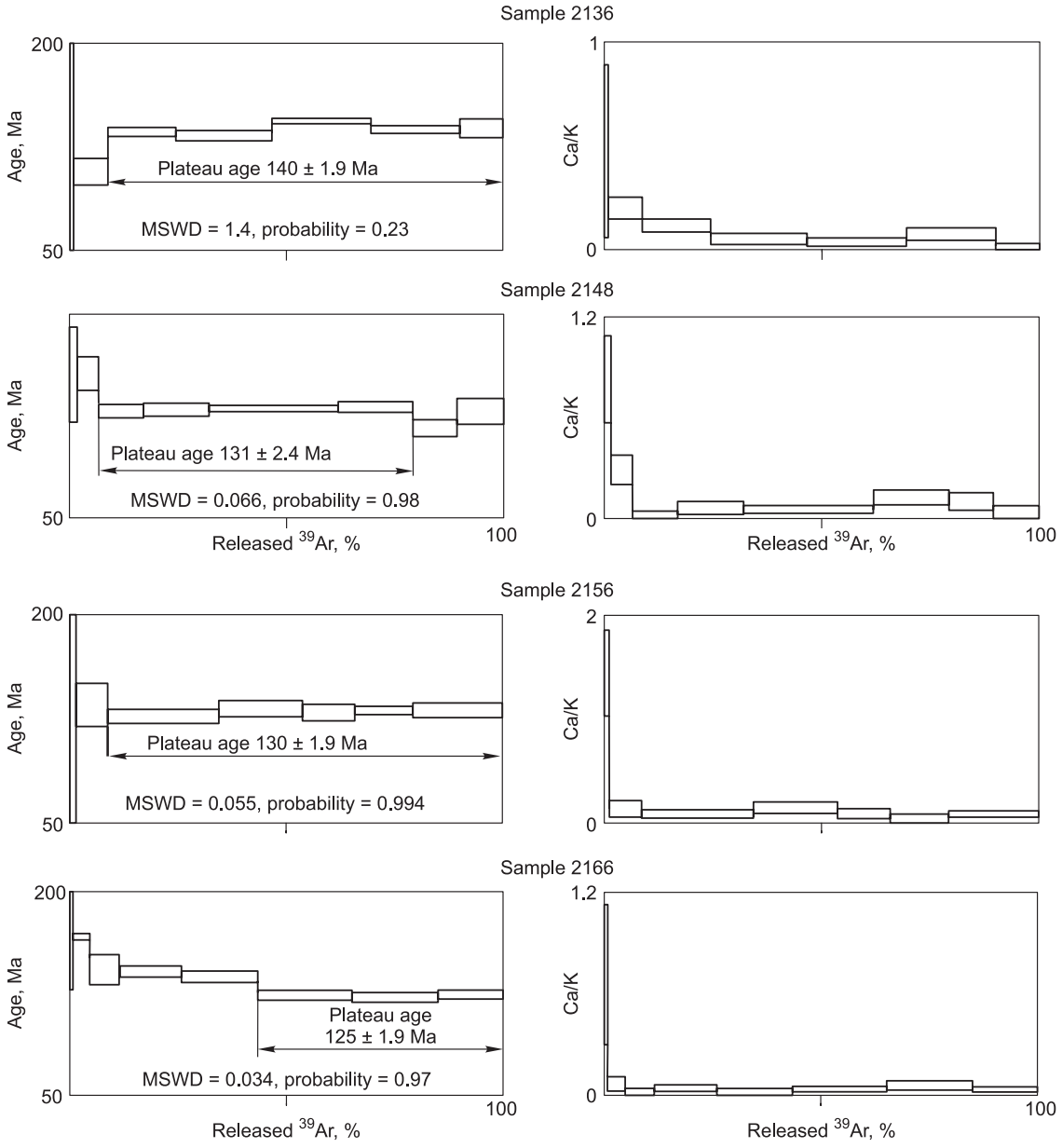

Fig. 6. Results of $^{40}Ar/^{39}Ar$ rock dating of monomineral fractions of phlogopite from nepheline syenites (sample 2136), feldspar from alkali syenites (samples 2148 and 2156) and feldspar of alkali granite (sample 2166) from the Yllymakh massif. The error is indicated with an interval of ±2σ.

125 Ma for sample 2166. The alkali syenites have negative ε_{Nd} values, which fall in a narrow interval between –13.07 and –14.09. The age of the syenite source $T_{Nd}(DM)$ = 1.7–2.0 Ga. The granites are characterized by a similar ε_{Nd} value (–13.06), but differ in model age $T_{Nd}(DM)$ = 1.4 Ga. On the other hand, the estimates of Nd model age calculated by the two-stage model $T(DM)$-2 for all species of the studied rocks are in the range between 2 and 2.1 Ga.

The rock samples 2134, 2140 and 2146 show close initial values $(^{87}Sr/^{86}Sr)_0$, which may indicate the homogeneity of the rock source. Alkali granites (sample 2166) show a significant enrichment of the radiogenic component, the primary ratio $(^{87}Sr/^{86}Sr)_0$ increases to 0.710 against 0.705 for the remaining samples. Such enrichment could be associated with the process of secondary rock change (high strontium mobility), but this fact is not confirmed by petrographic studies. It can be assumed that the source was contaminated with a substance enriched with radiogenic strontium.

In the $(^{87}Sr/^{86}Sr)_0 - \varepsilon_{Nd}(T)$ diagram, the rocks of the Yllymakh massif (Fig. 7), with the exception of alkali granites, fall into the range of values characteristic of high-potassium rocks of the Aldan shield: of the Central Aldan region (the following massifs: Tolmotian, Ryabinovyi, Yakokutsky, Zametny, Inagli), of the Verkhneamginskaya area and the Murunskyi massif. It should be noted that the values are located in the upper part of the region characterized by the

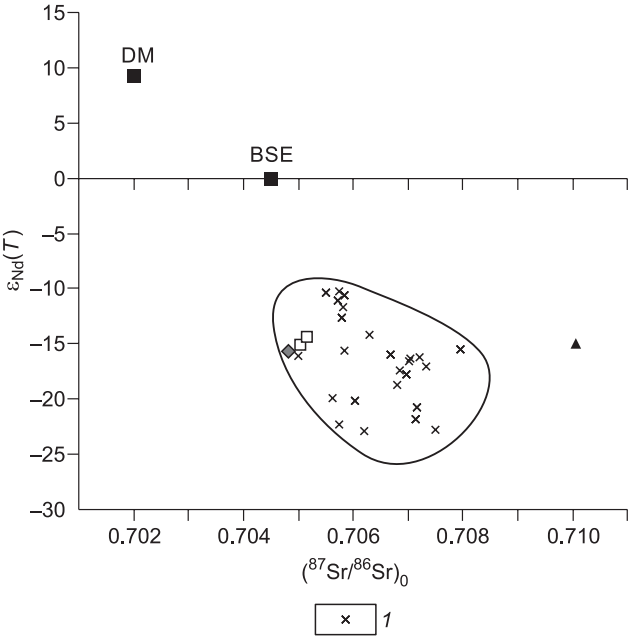

Fig. 7. The position of the studied rocks of the Yllymakh massif on the diagram $(^{87}Sr/^{86}Sr)_0 – \varepsilon_{Nd}(T)$ in comparison with high-potassium rocks of the Central Aldan and Verkhneamginsky geographical ranges of magmatism (Bogatikov et al., 1994; Mitchell et al., 1994; Davies et al., 2006). Symbols designations are in Fig. 3.

highest values of ε_{Nd} and contain relatively low amount of $(^{87}Sr/^{86}Sr)_0$ (Fig. 7).

DISCUSSION

Formation mechanism. The obtained petrographic, petrological-geochemical and geochronological data suggest that the massif was formed by several independent pulses of intrusion. The spectrum of rocks of the first two groups (feldspar and alkali syenites and feldspar syenites) was formed through a fractionation process according to the variation diagrams. The fractionating phases were both rock-forming phases (pyroxene, plagioclase), giving trends in the coordinates CaO– Na_2O–SiO_2 and MgO–Fe_2O_3–SiO_2, and accessory phases (apatite: P_2O_5–SiO_2) minerals. In this case, the sources of the melt of each pulse have similar geochemical parameters. The rocks are the same on the spectrum of alkalinity: potassium and potassium-sodium. In the variation diagrams, they form independent clusters only by silica content and, partially, by iron content. The shape of the geochemical spectra of granites, coinciding in shape and absolute values with the spectra of more melanocratic rocks, close to the content of K, Ti confirms the similarity of the melt sources from which the feldspar and feldspar syenites and granites crystallize. An additional evidence may be the similar ε_{Nd} values for all groups of rocks.

In addition to the similarities pointing to the syngenetic nature of the mantle source, the differences emphasizing the independence of magmatic pulses are noted. The main differences are in the divergence of petrochemical trends (for example, for Al_2O_3), in the behavior of individual scattered elements (Ba, Th, U, Sr), a significant difference between $^{87}Sr/^{86}Sr$ ratios in granites and syenites. The obtained geochronological characteristics also confirm the variant of pulse penetrations and the influence of the crustal contaminant on the rock-forming melt.

Based on the data obtained, as well as using the experience of previous researchers of alkaline rocks of the Central Aldan, it can be assumed that the mixing processes in crustal conditions are responsible for the emergence of a spectrum of rocks with the described material characteristics and it explains their genetic relationship. It is the mixing that gives the shift of the spectra of rare earth elements described above. At the same time, assimilation should occur with a material that does not carry a significant change in the isotopic composition of Nd, but only shifting the rare-earth spectra parallel to each other. One of the suitable options as assimilants can be highly siliceous rocks, perhaps even quartzites. The latter are widely distributed in the study area. According to the existing geological literature (Explanatory note…, 2016), the quartzites are a part of the Vasilyevskaya Formation of the Verkhnealdan group of Archean age. A possible objection to the melting temperature of relatively pure quartzites (under normal conditions it exceeds 1000 °C) can be eliminated by the fact that there would be no melting, but rather a dissolution of quartz rocks in a silicon unsaturated alkaline melt. The mixing mechanism is favored by the obvious correlation of rare-earth elements with silica.

On the other hand, the graphs of the rare-earth elements differ in form – they are even for feldspar and alkali syenites and U-shaped for the feldspar syenites and granites, and $^{87}Sr/^{86}Sr$ ratio in the granites, which is very different from that in the syenites, with the fact that the quartz is absolutely inert mineral in terms of accumulation of rare elements.

These details suggest a “dilution” of the rock-forming melt portions of the other of the melt, having a source with the same geochemical characteristics and an apatite in the restite, as the apatite has the highest distribution coefficients mineral/melt for the middle lanthanides (Sm, Eu, Gd, Tb) according to the database (https://earthref.org/KDD/). During a re-reactivation, with a partial melting of the source to a low degree, the apatite remains in the solid state, and the complementary melt will be depleted by the components included in it. Thus, the spectrum of rare-earth elements with U-shape can be obtained at similar values of ε_{Nd}. This variant is confirmed by a direct correlation of rare-earth elements (Sm, Eu, Gd, Tb) with P_2O_5 content in the studied rocks (Fig. 8).

Summarizing the above arguments, it can be assumed that the formation of the rock spectrum occurred by a reactivation of geochemically similar sources or one source formed by different degrees of melting with the addition of crustal material.

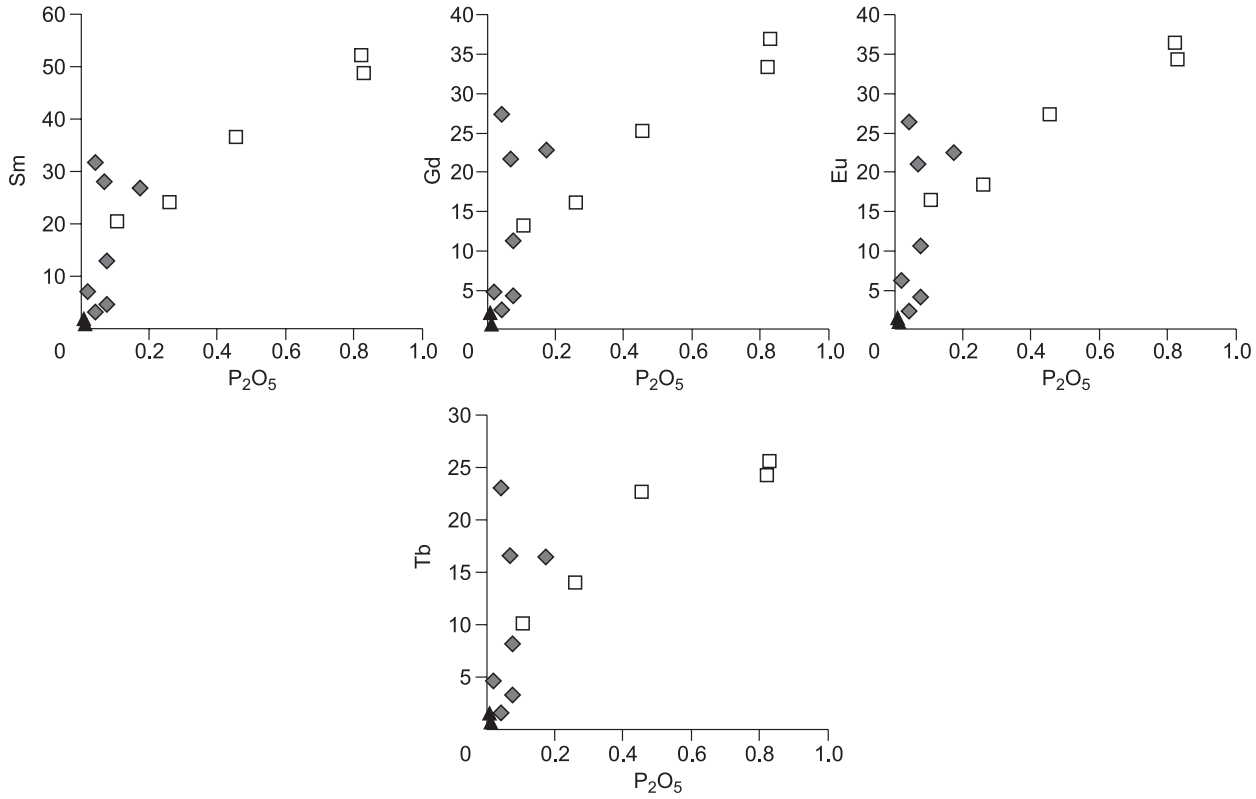

Fig. 8. Graphs of the ratio of the content of rare-earth elements (ppm) of the middle part of the spectrum with the content of phosphorus (weight percent) in the rocks of the Yllymakh massif. Symbols designations are in Fig. 3.

Source characteristics. The isotopic data obtained by us indicate that the formation of rocks occurred from a source with negative ε_{Nd} (about -15) and an increased $^{87}Sr/^{86}Sr$ ratio (~0.705). Previous researchers (Bogatikov et al., 1994; Mitchell et al., 1994) combine such isotope-anomalous characteristics of high-potassium rocks of the Aldan shield with the participation of an ancient subducted substance in the rock source. This, in addition to low ε_{Nd} values, can explain the high content of K, positive anomalies for a Pb, Nb-Ta minimum. However, it is necessary to take into account the abundance of Archean rocks with similar isotopic characteristics. According to (Explanatory note…, 2001), there are two formations among the Archaean rocks: Verhnesaldan and Fyodorovskaya, composed of metamorphic rocks. Petrochemical reconstruction suggests that the protoliths of these rocks were tholeiitic and calc-alkaline basalts, respectively. They have herewith ε_{Nd} characteristic values of (–33,7 for Verhnesaldansk and –16,8 for Fyodorovsk). It is most likely that already in the Archean time under the Aldan shield there was an enriched mantle source (Ariskin, 2015; Doroshkevich et al., 2018). Its reactivation in the Mesozoic time could cause the emplacement of alkaline rocks.

The time of formation of the massif and its geological position. To understand the geological position of the Yllymakh massif in the complex of Mesozoic rocks of Aldan province, we compared the obtained geochronological data on it with the data of other objects.

A typical object within the Central Aldan district is the Ryabinovyi massif (Kostyuk et al., 1990; Maksimov, 2003). On the basis of geological observations and radiological determinations on the Ryabinovyi massif, different age groups of alkaline and subalkaline rocks corresponding to four stages of intrusion formation were distinguished: T_3-J_1, J_1-J_2, J_3-K_1, K_1-K_2. The radiological age of sericite-microcline metasomatites within the Ryabinovoye ore field according to the K-Ar method is in the range between 134 and 120 Ma (Ugryumov and Dvornik, 1985; Dvornik, 2009). Modern ar-Ar dating data (Borisenko et al., 2011) showed that the main part of alkaline rocks (sills, rods, ring intrusions, volcanic series) was formed in the range between 160 and 135 Ma, while the formation of the dike complex: minettes, orthophyres, syenite porphyries, intrusion of alkaline picrites, shonkinites, and related rocks occurred in the later stages in the interval between 135 and 120 Ma. The U-Pb and Rb-Sr dating data confirm the above intervals (Shatov et al., 2012). The age of formation of rocks in the Ryabinovyi massif is in the range between 120 and 147 Ma, and this interval is the same as for the Aldan plutonic complex and for the Tobuk hypabyssal complex.

The formation of the alkaline frame of the Inagli massif also occurred in several stages (Ponomarchuk et al., 2019): (1) a crystallization of the dunite core margin – clinopyroxenites is dated no later than 142.4 ± 2 Ma; (2) formation of

the differentiated alkaline ring of the massif occurred in the range between 133 and 128 Ma: the age of crystallization of melanocratic syenites is 133.2 ± 2.2 Ma, formed by monzonite-porphyries – 130.8 ± 2 Ma, which is also confirmed by U-Pb datings (Ibragimova et al., 2015), of the leucocratic syenites – at least 128.2 ± 4.4 Ma, of the shonkinites – 128.4 ± 1.5 Ma.

Thus, the obtained interval of formation of the Yllymakh massif of 140–125 Ma coincides with the time of formation of the Ryabinovy massif and of the ring frame of the Inagli massif and is consistent with the model of global activation of this lithosphere area in the Early Cretaceous time.

SUMMARY

1. As a result of the research, three groups of rocks characterized by different mineralogical and petrographic features were identified: 1) feldspar and alkali syenites; 2) syenites from nepheline-containing to quartz-containing; 3) aegirine alkaline feldspar granites.

2. The analysis of petrochemical and geochemical diagrams showed the possibility of formation of the rock spectrum of two groups (feldspar syenites and alkali syenites) by fractionation of the melt in the course of the crystallization. The fractionating phases were both rock-forming phases (pyroxene, plagioclase), giving trends in the coordinates $CaO–Na_2O–SiO_2$ and $MgO–Fe_2O_3–SiO_2$, and accessory phases (apatite: $P_2O_5–SiO_2$) minerals.

3. The following sequence of formation of the variety of the studied rocks– feldspar syenites – alkali syenites (the first group) – alkali syenites – alkali granites is established. Three episodes of magma intrusion are determined – 140, 130 and 125 Ma. In each of the episodes, more acidic rocks were formed, having specific petrological and geochemical features on the one hand, but at the same time having similar characteristics on the other hand.

4. The isotopic composition of oxygen showed the predominance of mantle material in the source. The Nd and Sr isotopic data show that the rocks of the Yllymakh massif were formed in an enriched source. Sharply negative values of the ε_{Nd} of the studied rocks fit into the overall picture of the region – similar characteristics are determined for other objects of similar age (Inagli, Ryabinovyi, etc.).

5. All these results suggest that the formation of the rock spectrum occurred by reactivation of geochemically similar sources or a single source formed by different degrees of melting in the process of system evolution.

This work was performed within a state assignment of the project and with grants from the Russian Ministry of Education and Science (No. 5.2324.2017/4.6). Geochronological measurements were supported by the Russian Science Foundation, grant №19-17-00019.

REFERENCES

Ariskin A.A., Danyushevsky I.V., Konnikov E.G., Maas R., Kostitsya Yu.A., McNeill A., Meffre S., Nikolaev G.S., Kislov E.V., 2015. The Dovyren intrusive complex (northern Baikal Region, Russia): Isotope-geochemical markers of contamination of parental magmas and extreme enrichment of the source. Russian Geology and Geophysics (Geologiya i Geofizika) 56 (3), 411–434 (528–556).

Baksi, A.K., Archibald, D.A., Farrar, E., 1996. Intercalibration of $^{40}Ar/^{39}Ar$ dating standards. Chem. Geol., 129, 307 – 324

Bilibin, Yu.A., 1947. Petrology of Yllymakhskii Intrusive [in Russian]. Moscow, Leningrad.

Bilibin, Yu.A., 1958. Petrography of Aldan. Post-Jurassic intrusions of the Aldan region. Selected works [in Russian]. Academy of Sciences of USSR, Moscow. Vol. 1.

Bogatikov, O., Kononova, V., Pervov, V., Zhuravlev, D., 1994. Petrogenesis of Mesozoic potassic magmatism of the Central Aldan: A Sr-Nd isotopic and geodynamic model. Int. Geol. Rev. 36 (7), 629–644.

Borisenko, A.S., Gas'kov, I.N., Dashkevich, E.G., Okrugin, A.M., Ponomarchuk, A.V., Travin, A.V., 2011. Geochronology of magmatic processes and ore–formation in the Central Aldan gold-ore region. Int. Symp. Large Igneous Provinces of Asia. Irkutsk, pp. 38–39.

Bouvier, A., Vervoort, J.D., Patchett, P.J., 2008. The Lu–Hf and Sm–Nd isotopic composition of CHUR: Constraints from unequilibrated chondrites and implications for the bulk composition of terrestrial planets. Earth Planet. Sci. Lett. 273 (1–2), 48–57.

Chacko, T., Cole, D.R., Horita, J., 2011. Equilibrium oxygen, hydrogen and carbon isotope fractionation factors applicable to geological systems. Stable isotope geochemistry. Rev. Miner. 43, 1–81.

Davies, G.R., Stolz, A.J., Mahotkin, I.L., Nowell G.M., Pearson, D.G., 2006. Trace elements and Sr-Pb-Nd-Hf isotope evidence for ancient, fluid-dominated enrichment of the source of Aldan shield lamproites. J. Petrol. 47 (6), 1119–1146.

Doroshkevich, A.G, Prokopyev, I.R., Izokh, A.E., Klemd, R., Ponomarchuk, A.V., Nikolaeva, I.V., Vladykin, N.V., 2018. Isotopic and trace element geochemistry of the Seligdar magnesiocarbonatites (South Yakutia, Russia): Insights regarding the mantle evolution beneath the Aldan-Stanovoy shield. J. Asian Earth Sci. 154, 354–368.

Dvornik, G.P., 2009. Sericite-microcline metasomatites and ore-grade gold mineralization in Ryabinovsky ore field (Aldanian shield). Litosfera, No. 2, 56–66.

Dvornik, G.P., 2016. Metasomatism and Gold-porphyry Mineralization of Potassium Alkaline Massifs. Extended abstract Dr. Sci. in Geol. Mineral. Diss.

Dvornik, G.P., Elyuev, V.K., 2001. Geology, exploration and technological properties of vein-disseminated ores of Ryabinovy gold deposit, in: Scientific Basis and Advanced Technologies of Processing of Refractory Ores and Technogenic Raw Materials of Precious Metals: Writings of the International Conference [in Russian]. Publishing House UGGA, Yekaterinburg, pp. 128–129.

Epstein, S., Taylor, H.P., 1967. Variation of $^{18}O/^{16}O$ in minerals and rocks. Researches in Geochemistry. Abelson, P.H. (Ed.). Wiley, New York. Vol. 2, pp. 29–62.

Eremeev, N.V., 1984. Volcanic-Plutonic Complexes of Potassium Alkaline Rocks [in Russian]. Nauka, Moscow.

Explanatory note to the state geological map of the Russian Federation on a scale of 1:200 000, Aldan series, Sheet O-51-XVIII. E.P. Maksimov, E.B. Khotina (Eds.). Saint Petersburg, 2001.

Explanatory note to the state geological map of the Russian Federation on a scale of 1:1 000 000 (third generation). Aldan-Zabaikalsk series. Sheet O-52, 2016. Zelepugin V.N., Shkatova V.K. (Eds.). Saint Petersburg.

Fleck, R.J., Sutter, J.F., Elliot, D.H., 1977. Interpretation of discordant $^{40}Ar/^{39}Ar$ age–spectra of Mesozoic tholeiites from Antarctica. Geoch. Cosm. Acta 41, 15–32.

Goldstein, S.J., Jacobsen, S.B., 1988. Nd and Sr isotopic systematics of river water suspended material: implications for crystal evolution. Earth Plannet Sci. Lett. 87, 249–265.

Hoefs, J., 2009. Stable Isotope Geochemistry. Springer-Verlag, Berlin.

Ibragimova, I.K., Rad'kov, A.V., Molchanov, A.V., Shatova, V.V., Lepehina, E.N., Antonov, A.V., Tolmacheva, E.V., Solov'ev, O.L., Terekhov, A.V., Khorokhorina, E.V., 2005. Results of a U-Pb (SHRIMP II) dating of zircons from dunites of Inagli massif (Aldan shield) and the problem of genesis of concentric-zonary complexes. Regional Geology and Metallogeny, No. 62, 64–78.

Khomich, V.G., Boriskina, N.G., 2016. Nature of late Mesozoic ore-magmatic systems of the Aldan shield. Litosfera, No. 2, 70–94.

Khomich, V.G., Boriskina, N.G., Santosh, M., 2014. A geodynamic perspective of worldclass gold deposits in East Asia. Gondwana Res. 26, 816–833.

Khomich, V.G., Boriskina, N.G., Santosh, M., 2015. Geodynamics of late Mesozoic PGE, Au, and U mineralization in the Aldan shield, North Asian Craton. Ore Geol. Rev. 68, 30–42.

Kochetkov, A.Ya., 2006. Mesozoic gold-bearing ore-magmatic systems of Central Aldan. Russian Geology and Geophysics (Geologiya i Geofizika) 47 (7), 847–861 (850–864).

Kononova, V.A., Pervov, V.A., Bogatikov, O.A., Mus-Shumacher, U., Keller, I. 1995. Mesozoic potassium magmatism of the Central Aldan: Geodynamic and genesis. Geotechtonics 29, 224–234.

Kostyuk, V.P., Panina, L.I., Zhidkov, A.Ya., Orlova, M.P., Bazarova, T. Yu., 1990. Potassium Alkaline Magmatism of the Baikal-Stanovoi Rift-Related System [in Russian]. Nauka, Novosibirsk.

Maksimov, Ye.P., 1975. Experience of formation analysis of the Mesozoic magmatic formations on the Aldan shield. The Proceedings of The Academy of Sciences of USSR. Geological series. No. 4, pp. 16–32.

Maksimov, Ye.P., 2003. Mesozoic ore-bearing magmatogenic systems of the Aldan-Stanovoi shield. Extended abstract of Dr. Sci. in Geol. Mineral. Diss. [in Russian]. Yakutsk.

McDonough, W.F., Sun, S.-S., 1995. The composition of the Earth. Chem. Geol. 120, 223–253.

Mitchell, R.H., Smith, C.B., Vladykin, N.V., 1994. Isotopic composition of strontium and neodymium in potassic rocks of the Little Murun complex, Aldan Shield, Siberia. Lithos 32, 243–248.

Nikolayeva, I.V., Palessky, S.V., Kozmenko, O.A., Anoshin, G.N., 2008. Determination of rare-earth and high field strength elements in standard geological samples using the inductively coupled plasma mass spectrometry (ISP-MS). Geochemistry. No. 7, 1–6.

Panina, L.I., Nikolaeva, A.T., Rokosova, E.Yu., 2011. Crystallization conditions of the alkaline-basic dike from the Yllymakh Massif, Central Aldan: Evidence from melt inclusion data in minerals. Geochem. Intern. 49, 120–138.

Pervov, V.A., Kononova, V.A., Suddaby, P., Thirlwall, M.F., Frun, P., Bogatikov, O.A., Upton, B.G.J., Woolley, A.R., 1997. Potassium magmatism of the Aldan shield, Southeastern Siberia: as an indicator of multi-stage evolution of the lithospheric mantle. Petrology 5 (5), 415–430.

Ponomarchuk, A.V., Prokopyev, I.R., Svetlitskaya, T.V., Doroshkevich, A.G., 2019. $^{40}Ar/^{39}Ar$ geochronology of alkaline rocks of the Inagli massif (Aldan shield, southern Yakutia). Russian Geology and Geophysics (Geologiya i Geofizika) 60 (1), 33–45 (41–54).

Rokosova, E.Yu., Panina, L.I., 2013. Shonkinites and minettes of the Ryabinovyi massif (Central Aldan): composition and crystallization conditions. Russian Geology and Geophysics (Geologiya i Geofizika) 54 (6), 613–626 (797–814).

Rokosova, E.Yu., 2014. Composition and Features of Melt Crystallization during the Formation of Potassium Basite Rocks of the Central Aldan (on the Yllymakhsky, Ryabinovyi, and Inagli massifs). Extended abstract of PhD in Geol. Mineral. Dissert. [in Russian]. Novosibirsk.

Rokosova, E.Yu., Panina, L.I., 2013. Shonkinites and minettes of the Ryabinovyi massif (Central Aldan): composition and crystallization conditions. Russian Geology and Geophysics (Geologiya i Geofizika) 54 (6), 613–626 (797–814).

Sharp, Z.D., 1990. A laser-based microanalytical method for the in situ determination of oxygen isotope ratios of silicates and oxides. Geochim. Cosmochim. Acta 54, 1353–1357.

Shatov, V.V., Molchanov, A.V., Shatova, N.V., Sergeev, S.A., Belov, V.N., Terekhov, A.V., Radkov, A.V., Solovyev, O.L., 2012. Petrography, geochemistry and isotopic datings (U-Pb and Rb-Sr) of alkaline magmatic rocks of the Ryabinovy massif (Southern Yakutia). Regional Geology and Metallogeny, No. 51, 62–78.

Shatova, N.V., Skublov, S.G., Melnik, A.Ye., Shatov, V.V., Molchanov, A.V., Terekhov, A.V., Sergeev, S.A., 2017. Geochronology of alkaline magmatic rocks and metasomatites of the Ryabinovy stock (Southern Yakutia) based on zircon isotopic and geochemical (U-Pb, REE) investigations. Regional Geology and Metallogeny, No. 69, 33–48.

Shnai, G.K., Orlova, M.P., 1977. New data on the geology and potential gold content of Yllymakh massif (Central Aldan region). Geologiya i Geofizika (Soviet Geology and Geophysics) 18 (10), 57–65 (48–55).

Steiger, R.H, Jager, E., 1977. Subcommission on Geochronology: Convention on the use of decay constants in geo- and cosmochronology. Earth Planet. Sci. Lett. 36, 359–361.

Travin, A.V., 2016. Thermochronology of subduction-collision, collision events in Central Asia. Extended abstract of Dr. Sci. in Geol. Mineral. Dissert. [in Russian]. Novosibirsk.

Ugryumov, A.N., Dvornik, G.P., 1985. Sericite-microcline metasomatites of the Ryabinovyi alkaline massif (Central Aldan). Dokl. Acad. Nauk USSR 280 (1), 191–193.

Ugryumov, A.N., Dvornik, G.P., 1997. Petrochemical and chronological correlation of epileucite phonolites of the Polevskoy region of the Middle Ural, Northern Kazakhstan, Northern Baikal region, Aldan shield: New aspects of the minerageny of these rocks, in: Magmatism, metamorphism and deep structures of the Urals: Lecture notes of the 6th Ural Petrographical Conference. Part 2 [in Russian]. Ural Department of RAS, Yekaterinburg, pp. 55–57.

Ugryumov, A.N., Dvornik, G.P., Balakhonov, V.S., 1996. Metasomatic zonality and golden mineralization of the Yllymakh alkaline massif (Aldanian shield), in: The Proceedings of the Ural State Mining University. Series: Geology and Geophysics [in Russian]. Yekaterinburg. Issue 5, pp. 82–87.

Ugryumov, A.N., Dvornik, G.P., Balakhonov, V.S., 1996. Metasomatic zonality of the Mesozoic polygonal and polychronous Yllymakh gold ore node (Aldanian shield), in: The Proceedings of the Ural State Mining University. Series: Geology and Geophysics. Yekaterinburg. Issue 13, pp. 153–163.

Vladykin, N.V., 2005. Unique Murunsky massif of ultrapotassium agpaitic alkaline rocks and carbonatites: its magmatism and genesis, in: Genetical Types of Ore Deposits [in Russian]. Moscow, Issue 7, p. 20.

Yarmolyuk, V.V., Kovalenko, V.I., Ivanov, V.G., 1995. Intraplate late Mesozoic-Cainozoic volcanic province of Central-Eastern Asia – projection of the hot mantle field. Geotectonics 5, 41–67.

Yarmolyuk, V.V., Kovalenko, V.I., Kuzmin, M.I., 2000. North Asian superplume in Phanerozoic: magmatism and deep geodynamics. Geotectonics 5, 3–29.

https://earthref.org/KDD/

Editorial responsibility: A.E. Izokh